Jordan Journal of Civil Engineering, Volume **8**, No. **3**, **2014**

Experimental Investigation of Surface Pressure on '+' Plan Shape Tall Building

Souvik Chakraborty [1)]***, Sujit Kumar Dalui*** [2)] ***and Ashok Kumar Ahuja*** [3)]

[1)] Post Graduate Student, Department of Civil Engineering, Bengal Engineering and Science University, Shibpur, Howrah, India
[2)] Assistant Professor, Department of Civil Engineering, Bengal Engineering and Science University, Shibpur, Howrah, India
[3)] Professor, Department of Civil Engineering, Indian Institute of Technology Roorkee, Roorkee, India
E-Mails: csouvik41@gmail.com (S.Chakraborty), sujit_dalui@rediffmail.com (S.K. Dalui)

ABSTRACT

The variation in pressure distribution with change in wind orientation angle on different faces of a '+' plan shape tall building is studied in this paper. Experiments have been carried out with a rigid model in a boundary layer wind tunnel for wind incidence angles of 0˚ and 45˚. Peculiar pressure distributions on certain faces are observed. Moreover, drastic change in pressure distribution is observed for the two wind angles. Finally, the flow pattern around the model is computed using Computational Fluid Dynamics (CFD) package ANSYS CFX in order to explain the variation in pressure on different faces.

KEYWORDS: Wind tunnel testing, Interference effect, Mean pressure coefficient, Tall building, Wind incidence angle, Vortex shedding.

INTRODUCTION

Wind engineering is a wide ranging multi-disciplinary subject that has developed over the last few decades and is concerned with the effects of wind on the natural and built environment. These effects can be catastrophic, leading to the failure of major buildings or other structures or can lead to discomfort and disruption. Shortage of land around the world has given rise to construction of tall structures. Generally, these buildings are susceptible to wind load. The risk regarding wind load is even more for irregular plan shape buildings. Irregular flow around the building gives rise to dynamic behaviour of wind resulting from phenomena such as vortex shedding, buffering, galloping and flutter. Change in wind incidence angle may also lead to dynamic behaviour of wind. Although guidelines regarding pressure coefficients on regular plan shape buildings are available in international standards, *viz*. IS: 875 (part3) – 1987, AS/NZS: 1170.2 (2002), ASCE: 7-02 (2002), NBC (Part 4) (1995), the standards are mum regarding irregular plan shape buildings. Under wind action, a structure experiences two forces, *viz*. drag and lift. While drag gives rise to positive pressure, negative pressure (suction) is generated by lift.

Fair amount of research have already been carried out regarding tall buildings. Hayashida et al. (1990) studied the effect of different building plan shapes on aerodynamic force and displacement response of super high rise buildings. Davenport (1993) investigated the response of slender buildings when subjected to wind load. Thepmongkorn et al. (2002) studied the interference effect on wind induced coupled translational- torsional motion of tall buildings. The results indicated a significant increase in responses at

Accepted for Publication on 16/2/2014.

the critical wind speed where the frequency of the shed vortices originated from the interfering building coincides with the modal natural frequency of vibration of the principal tall building. Katagiri et al. (2002) discussed a spectral analysis method and a time history analysis method using motion-induced wind forces for wind responses of high-rise buildings with coupled across- wind and torsional vibrations. The results obtained by the two methods were quite close. Zhou et al. (2002) after investigating along wind load on tall buildings using different international codes suggested that the scatter occurring in calculation of wind load is mainly due to the variation in definition of wind load characteristics. As per Kim et al. (2008) findings, tapering effect has a more significant effect in across-wind direction than that in along-wind direction and wind-induced responses of a tapered building model are not always reduced compared to the responses of a basic building model of a square cross-section. Lin et al. (2004) based on the outcome of a wind tunnel study of nine square and rectangular models (1:500) suggested that crosswind and torsional response exceeds the along wind response for tall buildings. Balendra et al. (2005) compared the result of laser positioning measurement technique of wind induced displacement with outcomes obtained from conventional strain gauge method in the paper entitled "Direct Measurement of Wind Induced Displacement in Tall Buildings Using Laser Positioning Technique". Laser positioning technique was found to be quite accurate. Gomes et al. (2005) studied the effect of wind force on L- and U- shaped models for various wind angles ranging from 0˚ to 180˚. Huge difference was observed in wind pressure on 'U' and 'L' shaped models as compared to rectangular model. Fu et al. (2008) compared wind tunnel data with field measurements of storm response of two super tall buildings. The wind tunnel data showed good convergence with the field data. Kwok et al. (2009), after a survey of occupants of tall buildings, suggested that the priority of wind engineering is to build up rational occupant comfort serviceability criteria for super tall sensitive buildings. Gu et al. (2009) developed a new concept of "mode coupling factor" and a modified SRSS method for wind response and equivalent static wind load of complicated tall buildings. Amin et al. (2012) investigated the interference effects between two closely spaced buildings in geometric configuration of 'L' and 'T' shapes for various wind angles. Use of different interference factors for torsion and displacement was suggested.

However, most of the studies till date are on regular plan shape buildings. This paper focuses on the nature and magnitude of surface pressure coefficients on '+' plan shape tall building as obtained from wind tunnel test. In particular, this paper represents the variation in pressure coefficients on different faces of '+' plan shape tall buildings for wind incidence angles of 0˚ and 45˚.

Experimental Program

Flow Characteristics

The experiment was carried out in an open circuit wind tunnel under the boundary layer wind flow at Wind Engineering Center, Department of Civil Engineering (IIT Roorkee), India. The dimensions of the wind tunnel are 2.0 m (width) × 2.0 m (height) × 38.0 m (length). The experimental flow was simulated similar to that of terrain category 2 as per Indian standard for wind load IS: 875 (part 3) - 1987 at a geometric scale of 1:300. The velocity of wind in the wind tunnel was considered 10 m/s and turbulence intensity was 10%. The model was placed at a distance of 12 m from the upstream side (Fig. 1). The power-low index (α) for the velocity profile inside the tunnel is 0.133. A reference pitot tube is located at a distance of 7.8 m from the upstream side to measure free stream velocity during the experiment. Vertical profile of longitudinal velocity at the test section is given in Fig. 2.

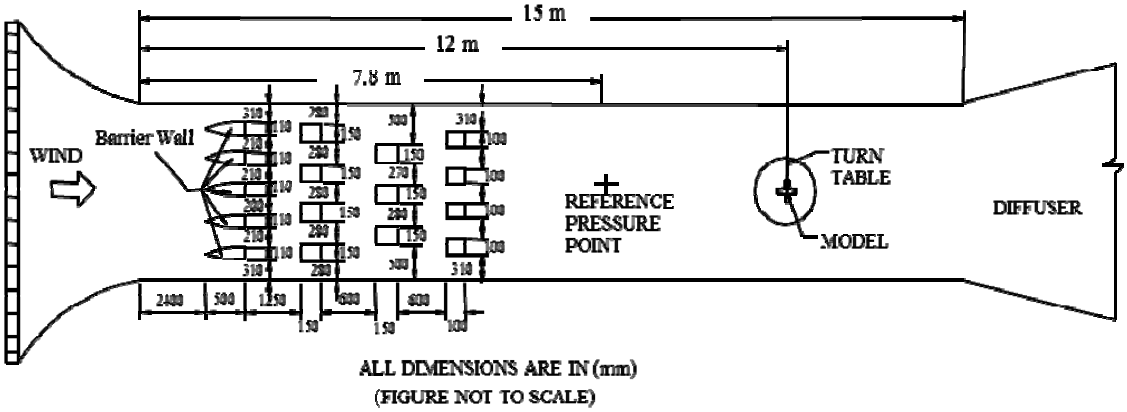

Figure (1): Position of model in wind tunnel (plan)

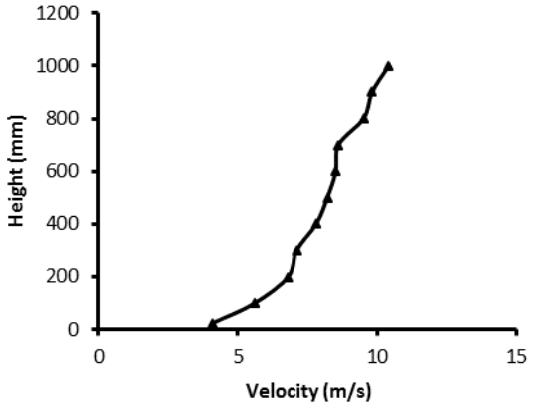

Figure (2): Variation of velocity in wind tunnel with height

Details of the Model

The model is made of a perspex sheet having a thickness of 4 mm. Dimensions of the model are 250 mm (width) × 250 mm (length) × 500 mm (height) (Fig. 3(a)). The dimensions of smaller faces of the '+' shape model are 50 mm (length) × 500 mm (height); whereas those of larger faces are 100 mm (length) x 500 mm (height). A total of 396 pressure tapping points were placed at nine different heights of 10, 30, 70, 150, 250, 350, 430, 470 and 490 mm (Fig. 3(b) and Fig. 3(c)). The pressure tapping points were kept near the wall boundaries in order to capture the high pressure variation occurring at the point of flow separation. The pressure tapings are made of steel tubing of 1 mm diameter and about 15-20 mm length. Pressure tapings are installed in the holes drilled in the form of a grid on all faces of the object building model.

Parametric Study

The '+' plan shape model was tested in the open circuit boundary layer wind tunnel for wind incidence angles of 0˚ and 45˚. Mean wind pressures on the all surfaces of the model were measured in order to study the pressure developed on such an irregular shape. Moreover, the effect of change in wind incidence angle was also studied.

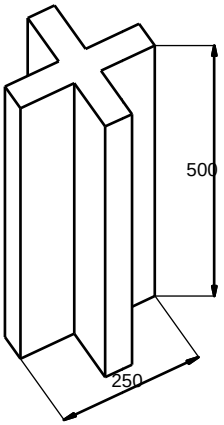

Figure (3 a): Isometric view of the model

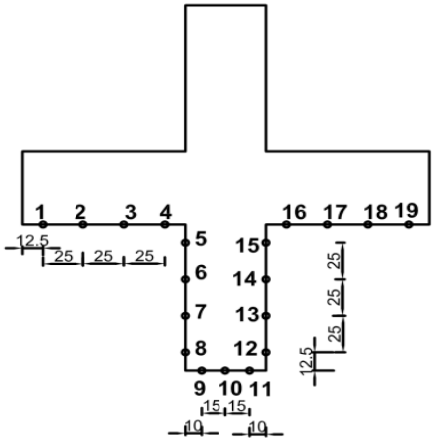

Figure (3 b): Model placed inside wind tunnel

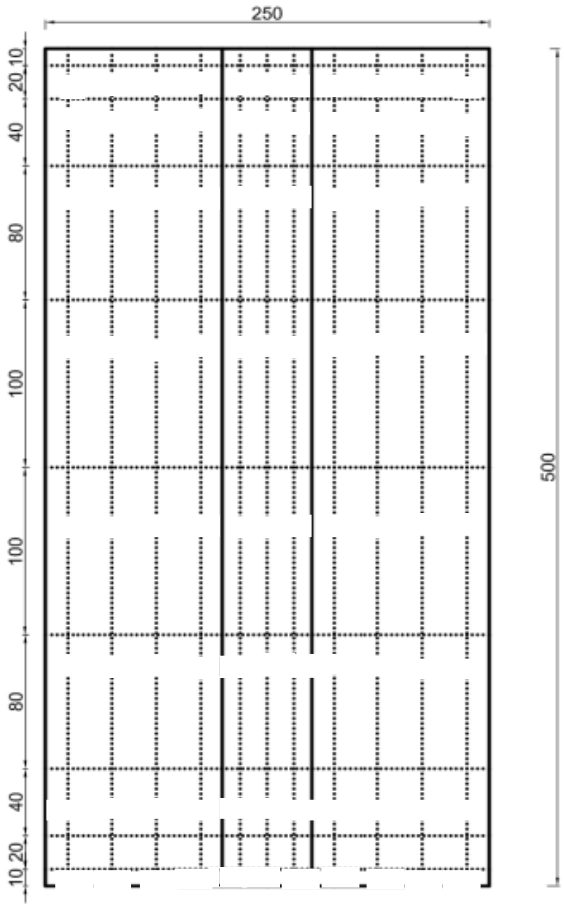

Figure (3 c): Plan and elevation of building along with pressure tapping points

Measurement Technique

First of all, the velocity profile was measured at the test section; i.e. at a distance of 12 m from the upstream side (without building model) with a free stream velocity of 10 m/sec. For this purpose, a second pitot tube was used. Then '+' building model of a total height of 500 mm was placed at a distance of 12 m (Fig. 2) from the upstream edge of the test section and wind pressure distribution on all surfaces of the object building was obtained through 396 pressure points using a pressure transducer and a data acquisition system for the above mentioned two wind incident angles.

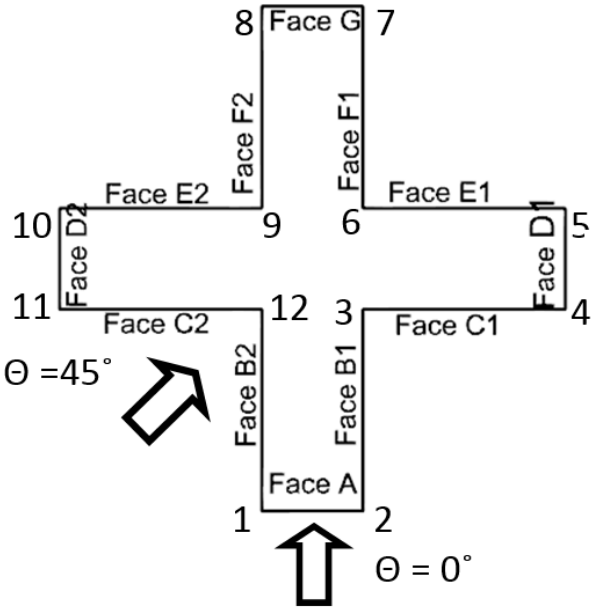

Figure (4): Wind incident angle(θ) with respect to different faces of the model

RESULTS AND DISCUSSION

Pressure Distribution

Fig. 4 shows the different faces of '+'plan shape model along with the two wind incidence angles. Pressure contours on all the faces are plotted with the pressure coefficients obtained from wind tunnel test for both wind angles.

Zero Degree Angle of Attack

The pressure contours on the symmetrical faces are identical and thus only 7 faces, *viz*. A, B1, C1, D1, E1, F1 and G, are sufficient to study the pressure distribution on the '+' plan shape model for 0˚ angle of attack. Fig. 5(a) – Fig. 5(g) show the pressure contour on various faces for the building model. The general characteristics of wind pressure on different walls are summarized as follows.

Face A is having a symmetrical pressure distribution about the vertical centerline with maximum pressure around the middle (Fig. 5(a)). The pressure is positive in nature with a magnitude of pressure coefficient varying between 0.42 and 0.86. The pressure decreases towards the edges. Unlike the case of rectangular buildings where side faces are subjected to negative pressure, faces B1 and B2 are mostly subjected to positive pressure. The pressure ranges between -0.2 and 0.95 with maximum pressure concentrated towards edge 2 (Fig. 5(b)). Negative pressure is observed in a small zone near the top surface. Face C1 is predominantly subjected to positive pressure with negative pressure near the top corner of edge 4. The pressure is concentrated towards edge 3 with a bubble of high positive pressure forming near the top (Fig. 5(c)). The pressure coefficient on face C1 varies between -0.1 and 0.75.

Fig. 5(d) shows the pressure distribution on face D1. Negative pressure; i.e. suction, is observed on face D1 with maximum pressure concentrated near edge 4. Pressure coefficient on face E1 varies between -0.25 and -0.46 with almost no variation along the horizontal line. The maximum suction pressure is concentrated near the top of edge 6 (Fig. 5(e)). Pressure on face F1 is concentrated towards edge 7 (Fig. 5(f)). Face G is also subjected to negative pressure with pressure coefficients varying between -0.26 and -0.43. Pressure distribution is symmetrical about the vertical centerline with almost no variation along the horizontal axis. The maximum pressure is concentrated near the top (Fig. 5(g)).

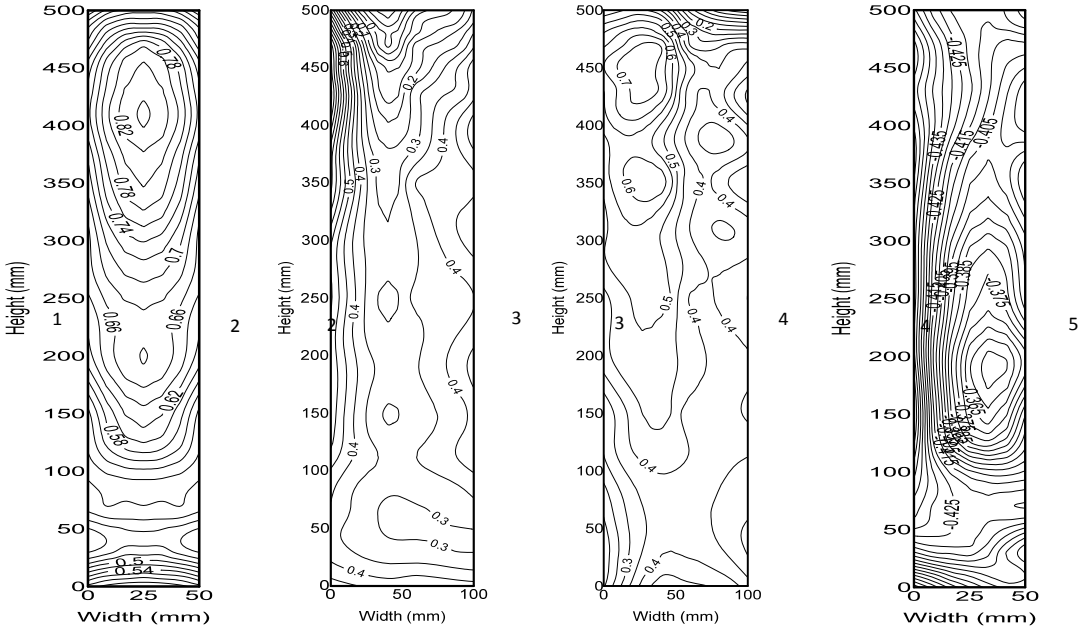

Figure (5 a): Pressure contour on face A for 0˚ wind angle

Figure (5 b): Pressure contour on face B1 for 0˚ wind angle

Figure (5 c): Pressure contour on face C1 for 0˚ wind angle

Figure (5 d): Pressure contour on face D1 for 0˚ wind angle

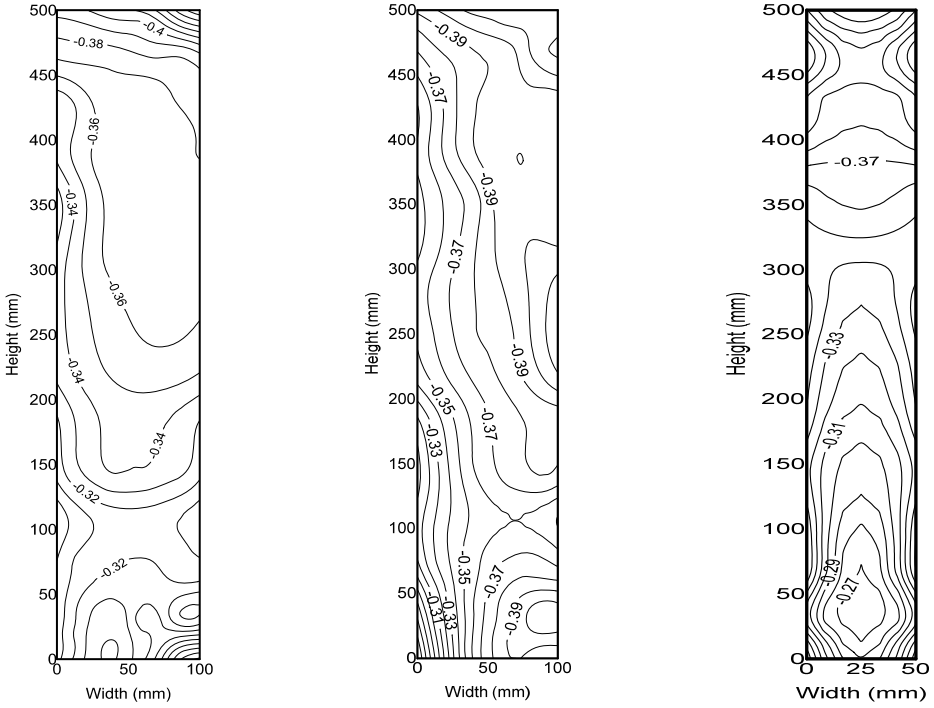

Figure (5 e): Pressure contour on face E1 for 0˚ wind angle

Figure (5 f): Pressure contour on face F1 for 0˚ wind angle

Figure (5 g): Pressure contour on face G for 0˚ wind angle

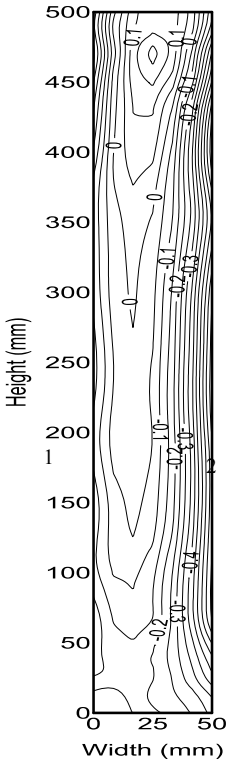

Figure (6 a): Pressure contour on face A for 45˚ wind angle

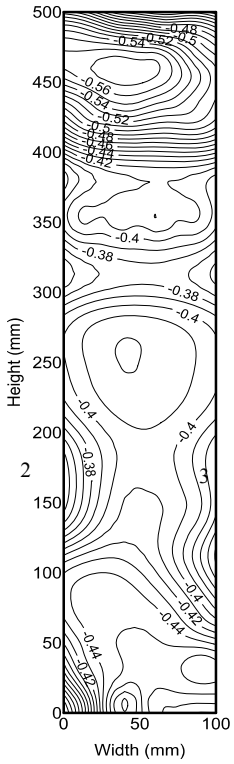

Figure (6 b): Pressure contour on face B1 for 45˚ wind angle

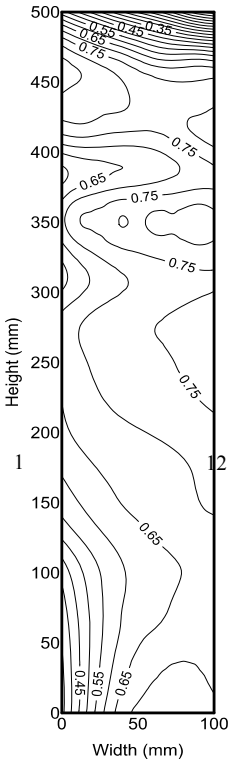

Figure (6 c): Pressure contour on face B2 for 45˚ wind angle

45˚ Angle of Attack

The pressure distribution in this case is also identical for symmetrical faces and thus only six faces are sufficient to study the pressure distribution on the model for 45˚ angle of attack. Fig. 6(a) – Fig. 6(f) show the pressure distribution on faces A, B1, B2, C1, D1 and E1, respectively. The general features of pressure on different walls are discussed below.

Unlike the case of 0˚ angle of attack, face A is predominantly subjected to negative pressure; i.e. suction, with a small bubble of positive pressure located near the top (Fig. 6(a)). The magnitude of pressure coefficient varies between -0.7 and 0.25 with maximum suction pressure concentrated near edge 2. Pressure coefficient on face B1 varies between -0.31 and -0.58 (Fig. 6(b)). A small bubble of high suction is observed near the top. Face B2 is subjected to positive pressure with maximum pressure near edge 12 (Fig 6(c)). The magnitude of maximum pressure coefficient on face B2 is 0.9. Face C1 is also subjected to negative pressure. A bubble similar to that on face B1 is formed near the top corner on face C1. Pressure distribution on face D1 is almost uniform (pressure coefficient of -0.33) with little variation near the edges (Fig. 6(e)). Fig. 6(f) shows the pressure distribution on face E1. The surface is subjected to suction varying over the small range from -0.15 to -0.4. The maximum pressure is concentrated towards the top of edge 6.

Comparative Study

The pressures generated on different faces of the '+' plan shape model due to the two wind angles are compared in order to have a better understanding of variation of pressure due to change in wind incidence angle. The key features observed are summarized below.

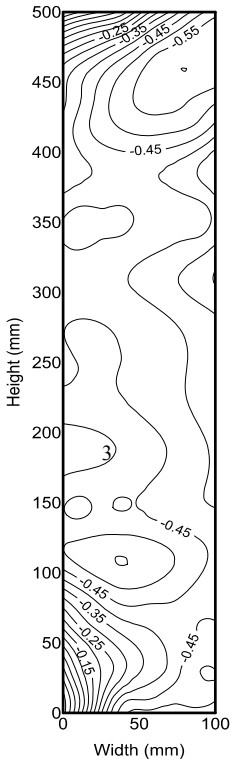

Figure (6 d): Pressure contour on face C1 for 45˚ wind angle

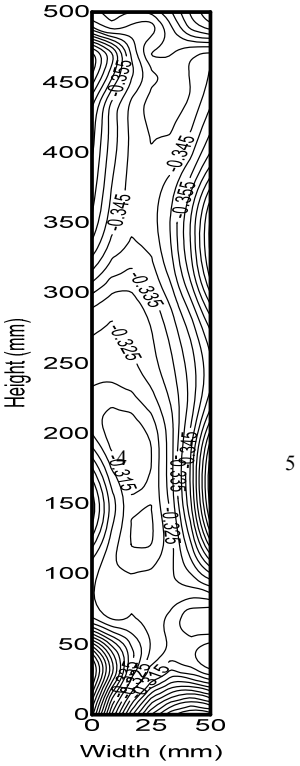

Figure (6 e): Pressure contour on face D1 for 45˚ wind angle

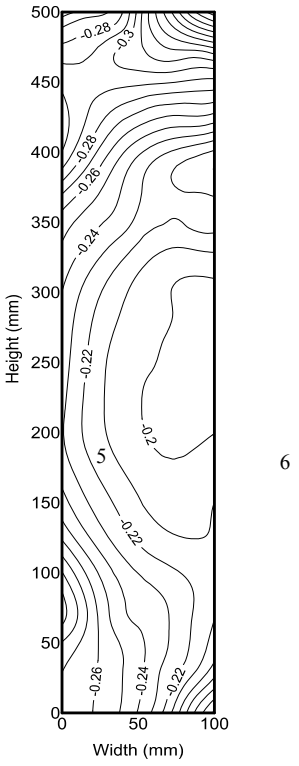

Figure (6 f): Pressure contour on face E1 for 45˚ wind angle

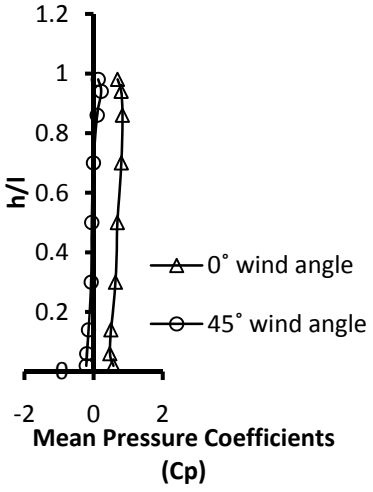

Figure (7): Comparison of pressure coefficients on face A along vertical centerline

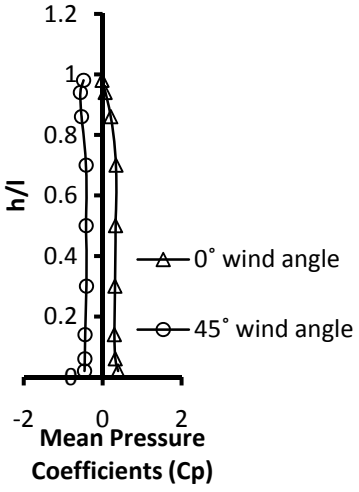

Figure (8): Comparison of pressure coefficients on face B1 along vertical centerline

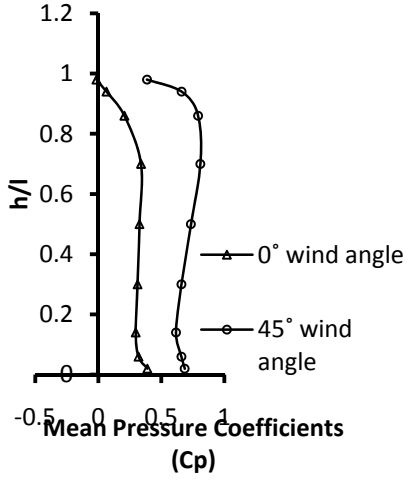

Figure (9): Comparison of pressure coefficients on face B2 along vertical centerline

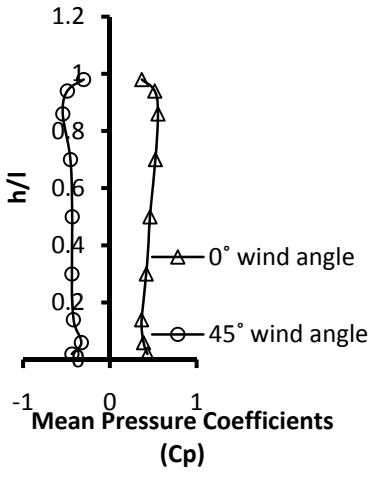

Figure (10): Comparison of pressure coefficients on face C1 along vertical centerline

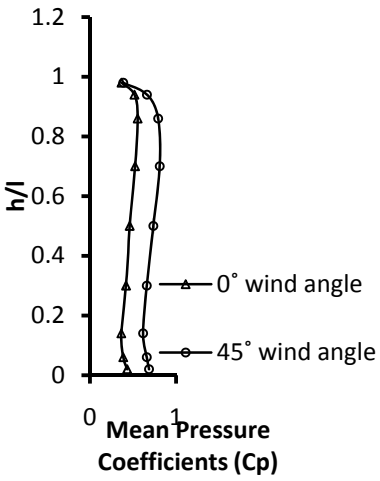

Figure (11): Comparison of pressure coefficients on face C2 along vertical centerline

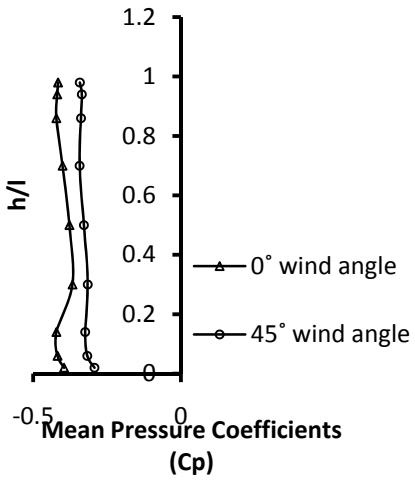

Figure (12): Comparison of pressure coefficients on face D1 along vertical centerline

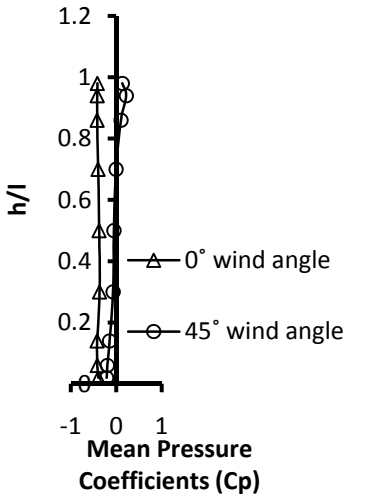

Figure (13): Comparison of pressure coefficients on face D2 along vertical centerline

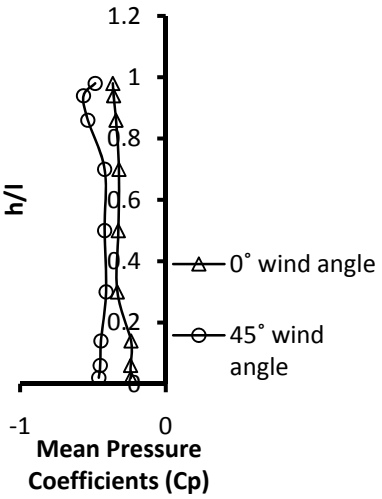

Figure (14): Comparison of pressure coefficients on face E2 along vertical centerline

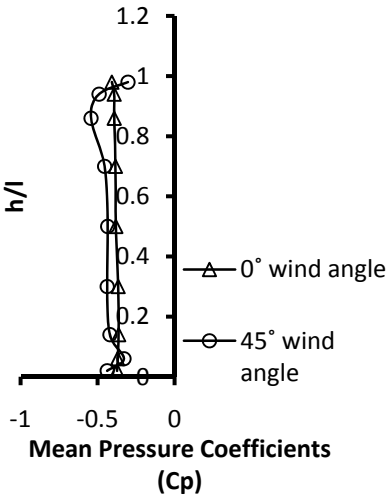

Figure (15): Comparison of pressure coefficients on face F2 along vertical centerline

Apart from the leeward faces, *viz*. E1, F1 and G, pressure variation occurs on all the faces with change in wind incidence angle. The comparisons of pressure coefficient for face G for the two wind angles are shown in Fig. 16. While for 0˚ wind incidence angle only positive pressure was observed on face A, both positive and negative pressures were observed for 45˚ wind angle (Fig. 7). The pressures on faces B1 and C1 are opposite in nature for the two wind incidence angles. With change in angle of attack from 0˚ to 45˚, the nature of pressure on the two faces changes from positive to negative (Fig. 8 and Fig. 10). The

magnitude of pressure coefficient on faces B2, C2, E2 and F2 increases for 45˚ wind incidence angle with maximum variation for face B2 being about 51% (Fig. 9). The maximum variations on faces C2, E2 and F2 are, respectively, 14%, 34% and 26% (Figs.11, 14 and 15). Again, the magnitude of pressure coefficient for faces D1 and D2 is less for 45˚ wind angle as compared to 0˚ wind angle. The maximum variation for face D1 is 15% while that for D2 is 9% (Figs. 12 and 13).

The variation along the horizontal centerline is shown in Fig. 17. While drastic variation is observed for faces A, B1, B2, C1 and C2, some minute difference is present for faces E1 and F1. The other faces have experienced more or less same pressure.

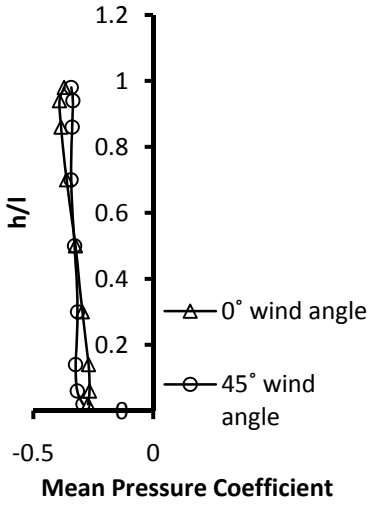

Figure (16): Comparison of pressure coefficients on face G along vertical centerline

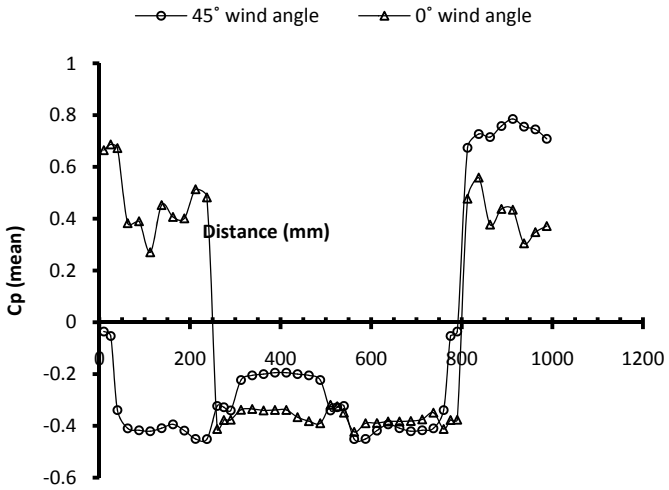

Figure (17): Comparison of pressure coefficients along horizontal centerline

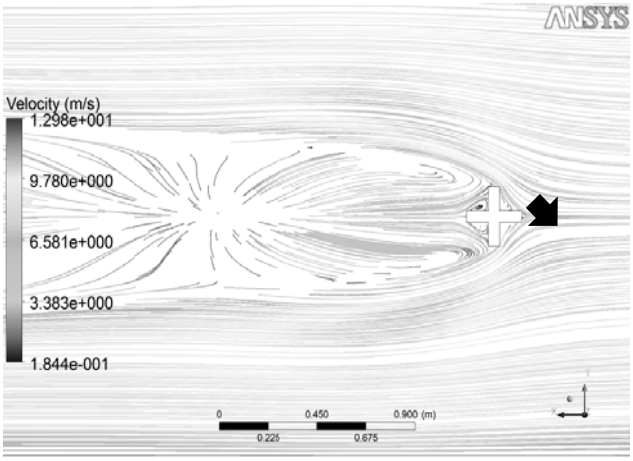

Figure (18): Flow around '+' plan shape model for 0˚ wind incidence angle

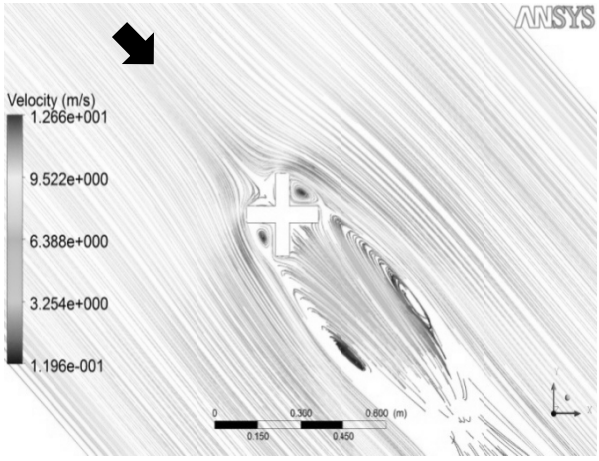

Figure (19): Flow around '+' plan shape model for 45˚ wind incidence angle

Flow Pattern

In order to investigate the cause behind the variation in surface pressure on the different surfaces of '+' plan shape tall building, the flow pattern is studied. ANSYS CFX is used to numerically model the building, and Shear Stress Transport (SST) viscosity model is used. Figs. 18 and 19 show the flow generated around the model for wind incidence angles of 0˚ and 45˚, respectively. In both cases, the wind sharply moves away from the edges of the windward side and reverts back after that. The flow pattern is symmetrical for both wind incidence angles and thus similar pressure behaviors are observed on the symmetrical faces. Two symmetrical vortices are formed on the leeward side in both cases. Two more vortices are formed in between faces B1, C1 and faces E2, F2 for 45˚ wind angle. Face A is facing the wind directly for 0˚ wind incidence angle and thus experiences positive pressure as observed from the pressure contours. Although faces B1 and B2 are expected to experience suction for 0˚ angle of attack, interference effect of Faces C1 and C2 induces positive pressure on both faces. The flow reverses after hitting faces C1 and C2 and results in generation of positive pressure on faces B1 and B2. Faces D1, D2, E1, E2, F1, F2 and G are subjected to negative pressure for 0˚ angle of attack. Apart from faces B2 and C2, all the other faces are subjected to negative pressure for 45˚ wind angle. The bubble of high suction formed at the top of faces B1 and C1 is due to the formation of vortex between the two faces (Fig. 19).

CONCLUSIONS

Wind tunnel study has showed that change in wind orientation may induce different pressures on various surfaces of a '+' plan shape building. The pressure may either increase or decrease depending on the location of a surface. The major findings of the present study are summarized below:

1. The symmetrical faces are having identical pressure distribution due to symmetry in wind flow for both wind angles.
2. For 0˚ wind incidence angle, faces B1 and B2 experience positive pressure due to interference effect of faces C1 and C2.
3. Apart from the two vortices on the leeward side, two more vortices are observed between faces B1, C1 and E2, F2 and result in the formation of a bubble of high negative pressure on the above limbs for 45˚ angle of attack.
4. For faces B2 and C2, an increase in magnitude of pressure coefficient is observed for 45˚ angle of attack as compared to 0˚ angle of attack.
5. The nature of pressure coefficient on faces A, B1 and C1 has reversed for 45˚ angle of attack. Positive pressure is observed for 0˚ angle of attack and suction for 45˚ angle of attack.
6. The magnitude of maximum pressure coefficient for face D1 has decreased for 45˚ angle of attack as compared to 0˚ angle of attack.
7. Faces E1, F1 and G are having identical values of pressure coefficient for both wind angles..

ACKNOWLEDGEMENT

The financial support for the experimental study from the Department of Science and Technology (DST), India is greatly appreciated and the work was fully supported by Wind Engineering Center (WEC) of IIT Roorkee, Roorkee, India.

REFERENCES

Amin, J. A., and Ahuja, A. K. (2012). "Wind-Induced Mean Interference Effects Between Two Closed Spaced Buildings." KSCE Journal of Civil Engineering, 16 (1), 119-131.

ANSYS 14.5, "ANSYS, Inc.", www.ansys.com

ASCE 7-02. (2002). "Minimum Design Loads for Buildings and Other Structures". American Society of Civil Engineering, ASCE Standard, Second Edition, Reston, Virginia.

AS/NZS 1170.2: 2002. (2002). "Structural Design Action, Part 2: Wind Actions". Australian/ New-Zealand Standard, Sydney, Wellington.

Balendra, T., Anwar, M.P., and Tey, K. L. (2005). "Direct Measurement of Wind-induced Displacements in Tall Building Models Using Laser Positioning Technique". Journal of Wind Engineering and Industrial Aerodynamics, 93 (5): 399-412.

BS 6399-2: 1997. (1997). "Loading for Buildings- Part 2: Code of Practice for Wind Loads". British Standard, London, UK.

Davenport, A.G. (1993). "The Response of Slender Structures to Wind". Wind Climate in Cities. Cermak et al. (Eds.), Germany, 209-239.

Fu, J. Y., Li, Q. S., Wu, J. R., Xiao, Y. Q., and Song, L. L. (2008). "Field Measurements of Boundary Layer Wind Characteristics and Wind-induced Responses of Super-tall Buildings." Journal of Wind Engineering and Industrial Aerodynamics, 96 (8-9), 1332-1358.

Gomes, M. G., Rodrigues, A. M., and Mendes, P. (2005). "Experimental and Numerical Study of Wind Pressures on Irregular-plan Shapes." Journal of Wind Engineering and Industrial Aerodynamics, 93 (10), 741-756.

Gu, M. (2009), "Study on Wind Loads and Responses on Tall Buildings and Structures". Seventh Asia-Pacific Conference, November 8-12, 2009, Taipei, Taiwan.

Hayashida, H., and Iwasa, Y. (1990). "Aerodynamic Shape Effects of Tall Buildings for Vortex Induced Vibration". Journal of Wind Engineering and Industrial Aerodynamics, 33: 237-242.

IS: 875 (Part 3). (1987). "Indian Standard Code of Practice for Design Wind Load on Buildings and Structures". Second Revision, New Delhi, India.

Katagiri, J., Ohkuma, T., and Marukawa, H. (2002). "Analytical Method for Coupled Across-wind and Torsional Wind Responses with Motion-induced Wind Forces". Journal of Wind Engineering and Industrial Aerodynamics, 90 (12-15), 1795-1805.

Kim, Y., You, K., and Ko, N. (2008). "Across-wind Responses of an Aeroelastic Tapered Tall Building". Journal of Wind Engineering and Industrial Aerodynamics, 96 (8-9), 1307-1319.

Kwok, K. C. S., Hitchcock, P. A., and Burton, D. (2009). "Perception of Vibration and Occupant Comfort in Wind-excited Tall Buildings". Journal of Wind Engineering and Industrial Aerodynamics, 97 (7-8), 368-380.

Lin, N., Letchford, C., Tamura, Y., and Liang, B. (2004). "Characteristics of Wind Forces Acting on Tall Buildings". Journal of Wind Engineering and Industrial Aerodynamics, 93, 217-242.

NBC (Part 4). (1995). "Structural Commentaries". National Research Council of Canada.

Simiu, E., and Scanlan, R.H. "Wind Effects on Structures". 2nd edition, John Wiley and Sons, New York.

Stathopoulos, T., and Baniotopoulos, C.C. (2007). "Wind Effects on Buildings and Design of Wind-Sensitive Structures". Springer, Wien, New York, Udine, Italy.